# Extreme high temperature events in the Northwest Pacific under global warming

**Zhiwei Chen**[a,*], **Jiancheng Kang**[b], **Guodong Wang**[c]

[a] School of Business, Shanghai Normal University TianHua College, Shanghai 201815 China
[b] School of Environmental and Geographical Sciences, Shanghai Normal University, Shanghai 200234 China
[c] Academic Affairs Office, Shanghai Institute of Tourism, Shanghai 201418 China

*Corresponding author, e-mail: 546335462@qq.com

**ABSTRACT**: Variation characteristics of the extreme high temperature events and their relationship with El Niño-Southern Oscillation (ENSO) in the Northwest Pacific were analyzed, utilizing the National Oceanic and Atmospheric Administration (NOAA) Daily Sea Surface Temperature (SST) Analysis Data during 1982–2014. The results indicated that extreme high temperature events mainly occurred during the months of June to October, and the frequency of such events was increasing, i.e. the number of days of extreme high temperature events and the duration of single extreme high temperature events increased gradually. The extreme high temperature events showed high and low frequency oscillations in the 1–4a and 4–7a cycles, and the main cycle scale was 3–5a. The SST of the Northwest Pacific was linearly related to the intensity of ENSO. In the second half of the year (June to December), the ENSO index of the Nino3.4 areas was significantly and negatively correlated to the extreme high temperatures. This meaned that the extreme high temperature events were likely to occur when the Pacific equatorial cold phase (La Niña event) occurred in the ENSO Cycle. The trade wind anomaly over the equatorial Pacific Ocean and the massive air-sea interactions in the ENSO Cycle had an important impact on the extreme high temperature events in the Northwest Pacific. It is hoped that the results obtained from this work will lay the foundation for monitoring and forecasting extreme weather and climate events.

**KEYWORDS**: extreme high temperature events, El Niño and La Niña events, ENSO, Northwest Pacific

## INTRODUCTION

The Intergovernmental Panel on Climate Change (IPCC 2011) pointed out that extreme weather and climate events have changed since 1950. What is certain is that, on a global scale, it has been observed that the number of colder days and nights on most of the lands is decreasing, while the number of warmer days and nights is increasing [1]. However, there are few observations and studies on the changes of extreme SST events in the ocean. Thomas et al found out that over the past few decades, Marine Heatwaves (MHWs) have lasted longer with higher frequency, greater range, and greater intensity; and this trend will be accelerated as global warming intensifies [2]. Studies have shown that the El Niño occurring in the Tropical Pacific Ocean and the Southern Oscillation occurring in the atmosphere are intrinsically interrelated large-scale air-sea interaction events, and they are of the same phenomena's heterophony in two media. El Niño

and the Southern Oscillation are collectively called ENSO [3, 4]. Because of the interaction between the ocean and the atmosphere and the complexity of the interaction, ENSO has obvious characteristics of circulating phenomenon, which is also known as the ENSO Cycle; and the El Niño and the La Niña are the two extremes in the ENSO Cycle Phases, i.e. warm and cold phases of the Cycle [5].

Many researches have been done on the interaction between ENSO and sea-atmosphere [6–14]. The oceanographic model, which was proposed in the 1970s, completely described the oceanic phenomena and evolution of the El Niño phenomenon near the Equator [6]. Huang et al used the study of the coupled model of the sea-atmosphere to point out that the circulation anomalies caused by the warming of the warm pool in the Northwest Pacific and the westerly anomalies over the Western Equatorial Pacific would have an important impact on the development and attenuation of the El Niño and the La Niña events [7]. Bejarano et al pointed out that

the processes of vertical advection of the subsurface SST anomaly formed by the upwelling process and the SST zonal advection caused by the anomalous ocean current effectively controlled the development of ENSO and the transition of its phases [8]. It has also been pointed out that there was a significant positive correlation between interannual variability of SST over the Equatorial Indian Ocean and the East Pacific, and there was an intrinsic physical connection between ENSO-associated changes in the Indian Ocean and ENSO [9]. In addition, Kug et al pointed out that warming of the Indian Ocean SST, as one of the features of the El Niño, would have a negative feedback on ENSO [10]. This negative feedback affected obviously on the El Niño events, and subsequently on the La Niña. Regarding changes in ENSO intensity in the context of global warming, some scientists observed that the intensity of the El Niño has increased over the past 30 years [11–13]. Cai et al showed that warming of the Equatorial Central and Eastern Pacific caused increases in the frequency of extreme ENSO events after global warming [14].

The Northwest Pacific is a key area that affects China's climate change. Utilizing the NOAA SST data to determine the threshold of extreme temperature, the temporal and spatial variation characteristics of extreme temperature events in the Northwest Pacific during the last 33 years were discussed in this study. A variety of statistical diagnostic methods were used in the discussion.

## MATERIAL AND METHODS

### Data

A set of NOAA SST Data (1982.01–2014.12, 0° to 30°N, 105° to 155°E, spatial resolution: 0.25° × 0.25°, and temporal resolution: 1 day) consists of two data products from different satellite data: Advanced Very High Resolution Radiometer (AVHRR) and Advanced Microwave Scanning Radiometer (AMSR) ftp://eclipse.ncdc.noaa.gov/pub/OI-daily-v2/netcdf-uncompress. The temporal and spatial resolutions of the two data products are significantly higher than that of the previous 1° × 1° degree weekly average analysis data (https://www.nodc.noaa.gov/OC5/WOD/pr_wod.html). The AVHRR data are in good agreement with the field observation data, and the use of infrared and microwave tools also reduces the systematic errors [15].

### Methods

The daily average temperature calculation, extraction of two-dimensional grid data (excluding the data of null values), and the average daily temperature of research areas are obtained by calculating the arithmetic average values.

*Determination of extreme values and extreme thresholds:* Confirmation of extreme weather events could be based on experience, or significant impact on society and economy. But for a quantitative study, we determined a threshold from the view point of meteorology. The Fourth IPCC Report was based on the probability distribution of meteorological elements [16], and defined events less than or equal to the 10th (i.e. greater than or equal to the 90th) percentile as extreme events [17]. In the study of extreme climate events, some scholars also took the 5/95th percentile value as the extreme value threshold [18–23].

In this study, the daily average temperatures were arranged in ascending order, then the Percentile Function was used to calculate the 10th/90th percentile as the threshold of extreme temperatures. When the SST of a certain day was higher than 90% threshold, it was defined as extreme high temperature day.

The monthly, annual, decadal, periodic, and spatiotemporal evolutions of extreme high temperature events and their relationship with ENSO in the Northwest Pacific over the past 33 years were analyzed using empirical orthogonal function decomposition, Morlet wavelet analysis, power spectrum analysis, 4th degree polynomial fitting, and linear inclination rate.

*Empirical orthogonal function (EOF) analysis steps were as follows:* Preprocessing and transforming data to anomaly forms, then a matrix of data $X_{m \times n}$ could be obtained;

Computing the intersection product of matrix $X$ and its transposed matrix $X^{\mathrm{T}}$;

$$C_{m \times m} = \frac{X X^{\mathrm{T}}}{n} \quad (1)$$

Computing characteristic roots $(\lambda_1, \ldots, \lambda_m)$ and mode $(V_{m \times m})$ of matrix $C$;

$$C_{m \times m} V_{m \times m} = V_{m \times m} \Lambda_{m \times m} \quad (2)$$

Computing principal components by projecting EOF into matrix $X$ and obtaining all time-varying coefficients (principal components);

$$PC_{m \times n} = V T_{m \times m} X_{m \times n} \quad (3)$$
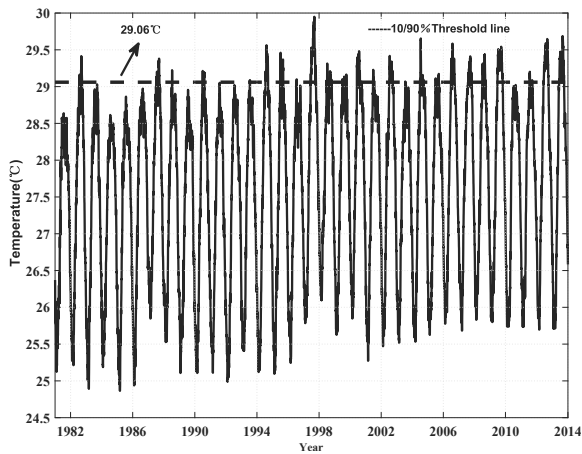
**Fig. 1** The average daily temperature variation in the Northwest Pacific.

Performing significance test and computing the error range of characteristic roots, $\lambda$;

$$e_j = \lambda_j \left(\frac{2}{n}\right) \frac{1}{2} \qquad (4)$$

A continuous wavelet transforms with a discrete time series $x_n$ ($n = 1, \ldots, N$) of equal time step $\delta t$ could be defined as a wavelet function $\psi$ scaling and a convolution of $x_n$ under conversion;

$$W_{n'}^x(s) = \sqrt{\frac{\delta t}{s}} \sum_{n=1}^{N} x_n \psi^* \left[\frac{(n'-n)\delta t}{s}\right] \qquad (5)$$

Obtaining the wavelet power spectrum by transforming the wavelet scale $s$ and localizing along the time index $n'$, a map showing the fluctuation characteristics of the time series at a certain scale and its variation with time.

Defining the Fourier power spectrum of AR1 processed by *lag-1* autocorrelation $\alpha$;

$$P_k = \frac{1-\alpha^2}{|1-\alpha\,e^{-2i\pi k}|^2} \qquad (6)$$

where $k$ is the Fourier frequency index, usually estimated in the study at a significant level of 5% on each scale.

**RESULTS AND DISCUSSION**

With the 90th percentile, the extreme high SST threshold was 29.06 °C (Fig. 1). The daily average sea surface temperature over the years in the Northwest Pacific was 27.59 °C, and the average sea surface temperature showed a gradual upward trend with an increase of 0.22 °C/10a. Moreover,

**Table 1** Average monthly occurrence of extreme temperature events in the Northwest Pacific during 1982–2014.

| Month | Number of days | Percentage |
|---|---|---|
| June | 154 | 12.72 |
| July | 367 | 30.31 |
| August | 332 | 27.42 |
| September | 298 | 24.61 |
| October | 60 | 4.95 |
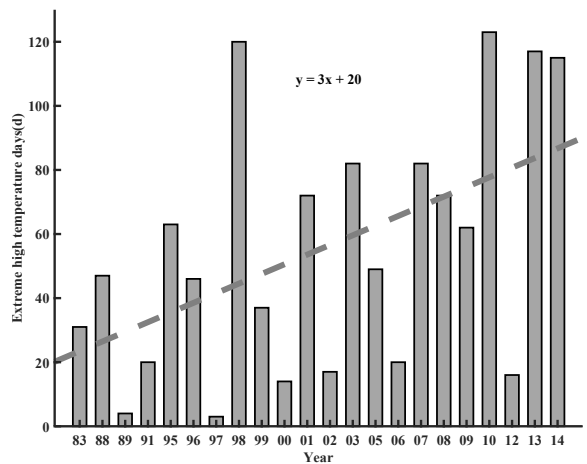


**Fig. 2** The distribution of extreme high temperature days in the Northwest Pacific.

as shown in Fig. 1, the extreme high temperature ranged from 29.06 to 29.95 °C. The maximum sea surface temperature appeared on September 7, 1998, was 2.36 °C above the daily average temperature over many years.

Table 1 shows the monthly occurrence of extreme temperature events during 1982–2014. It could be seen that the extreme high temperature events mainly concentrated during June–October, of which July accounted for 30.31%; and the proportions in August, September and June were 27.42%, 24.61% and 12.72%, respectively. The proportion in October only accounted for 4.95%.

The number of days experiencing extreme heat from 1982 to 2014 in the Northwest Pacific was 1211 (Fig. 2), with an average of 36.7 days per year. The number of extreme high temperature days varied greatly. The least extreme high temperature events occurred in 1997 (3 d), and the most occurred in 2010 (123 d). It shows an overall linear increase trend (30 d/ 10a). As seen from Fig. 1, the frequency of extreme high temperature events increased significantly. In the 1980s, the occurrence cycle of extreme high temperature events was 2–4
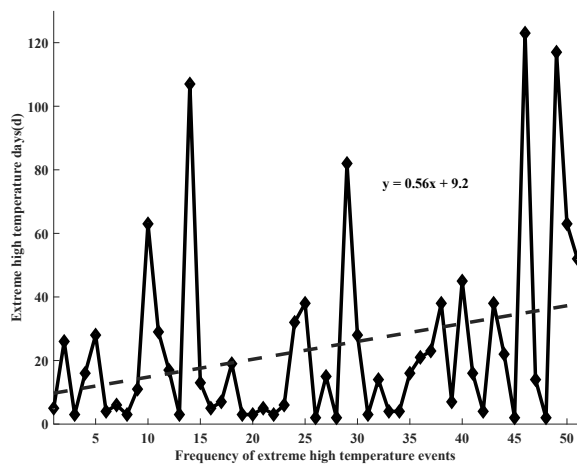
**Fig. 3** The duration of a single extreme SST event.

years. However, in the 1990s, such the occurrence cycle was 1–4 years. In the 21st century, it occurred every year except 2004 and 2011, which showed that the extreme high temperature events were increasingly frequent.

From 1982 to 2014, a total of 51 extreme SST events occurred in the Northwest Pacific and the average duration was 25 days; and the longest and shortest durations were 123 and 2 days, respectively (Fig. 3). In the years 1998, 2010, and 2013, the duration of a single high temperature event exceeded 100 days. In the recent 33 years, the duration of a single extreme high SST event showed a weak linear increase, with an increase rate of 0.56 days/time. By general, both the average and the maximum SST of the single extreme high temperature event in the Northwest Pacific showed a slight uptrend. The average rate of temperature rises was 0.032 °C/time, and the maximum SST rising rate was 0.049 °C/time.

To further discuss the periodic variation characteristics of the extreme temperature events from 1982 to 2014, the time series of extreme temperature events were analyzed using Morlet wavelet transform and wavelet power spectrum (Fig. 4). Fig. 4a shows the annual change cycle of extreme high SST events; and Fig. 4(b–f) show the change periods for the months of June–October, respectively. From Fig. 4a, we could see that the periodic scales of 95% confidence test in the year of high temperature were 1–4a and 4–7a, and the time of the 1–4a and the 4–7a periodic scales were 1992–2006 and 2007–2014, respectively. In Fig. 4(b–f), during the period from June to October when the extreme high temperature events occurred, the

change periods of 1–4a and 4–7a were also exhibited, and the wavelet full spectrum test passed the 95% confidence level. The main cycle scale was 5a. In summary, it could be seen that the extreme high temperature events in the Northwest Pacific showed high and low frequency oscillations of 1–4a and 4–7a, with a main period of 3–5a.

EOF analysis was used to analyze the SST from 1982 to 2014. The advantage of this method was that the form of orthogonal function could be determined according to the main features of SST field, and the spatial distribution of each feature vector and its time series changes could be obtained for exploring the temporal and spatial variations of SST in the past 33 years.

The EOF decomposition of the SST in the Northwest Pacific showed the variance contribution rates of the four modes, and the cumulative variance contribution rate was 84.38%, which could represent the main characteristics of the original field. Among them, the first modal variance contribution rate reached 55.84%, reflecting the main distribution characteristics and trend of SST in the recent 33 years in the Northwest Pacific. Therefore, this study only analyzed the first mode.

Fig. 5 shows the spatial distribution of the first mode. It could be seen that the first mode was positively correlated throughout the studied area, indicating that the SST variation trend in the Northwest Pacific had good overall consistency in space, and the Northwest Pacific warming and cooling in this mode was in the same phase. From the spatial distribution, the larger SST variability was located in the East China Sea, followed by the warm pool area in the Northwest Pacific, indicating that the East China Sea and the Northwest Pacific warm pool were the areas where the most significant SST changes happened in the Northeast Pacific.

To study the relationship between the SST anomalies in the Northwest Pacific and ENSO events, the correlation between the first modal time coefficient and Nino3.4 Index was analyzed. To remove the interference of high-frequency signals, such as seasonal and annual signals, the first modal time coefficient and the Nino Index were calculated using a low-pass Gaussian filter with 5-year cutoff. The results are shown in Fig. 6. Correlation analysis showed that the correlation coefficient of SST anomalies in the Northwest Pacific and Nino3.4 Index was −0.62 (over 99% significance test). It could be seen that the intensity of SST in the Northwest Pacific was linearly correlated with the intensity of ENSO. Hence, in the Northwest Pacific, the SST
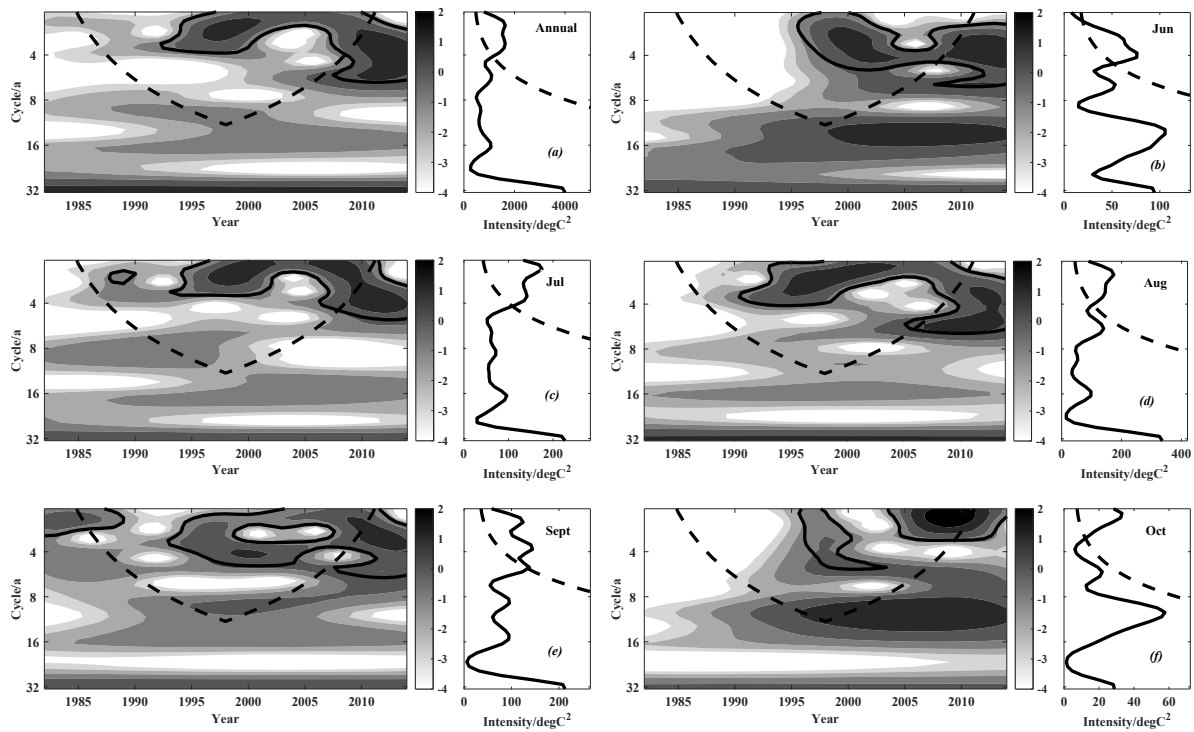
**Fig. 4** Wavelet power spectrum variation of the number of days of extreme high SST events.
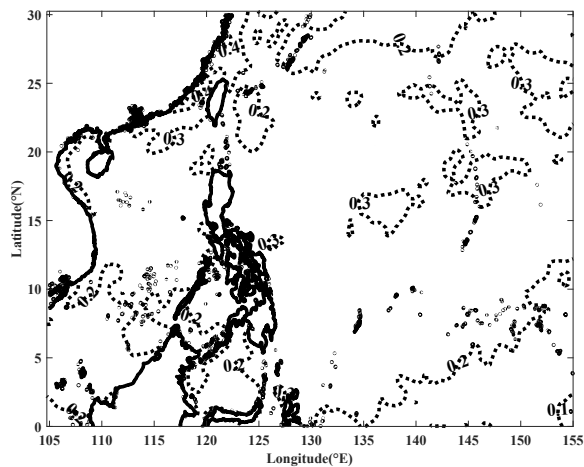


**Fig. 5** Spatial distribution of the first mode of the EOF SST in the Northwest Pacific.
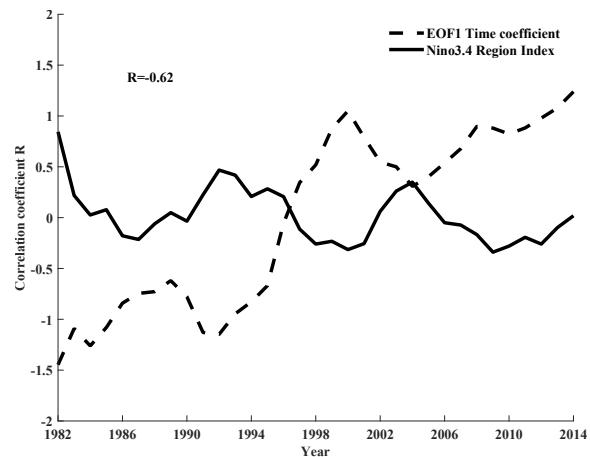


**Fig. 6** Comparison between the first modal time coefficient curve and Nino3.4 Region Index.

decreased significantly during the El Niño event, while the SST increased significantly during the La Niña event.

Comparing the SST spatial distributions of July, August and September in extreme year events with the normal years, it was found that in the year of extreme high temperature event, the warm pool temperature in the Northwest Pacific was obviously

higher than that in normal years; and the distribution of the warm pool was broader and extended to higher latitudes; and it was most obvious in the center of the warm pool, east of the Philippines.

In order to explore the relationship between the ENSO events and the Northwest Pacific extreme temperature events from 1982 to 2014, this study used the SSTA Index of NINO 1+2+3+4 as the basis
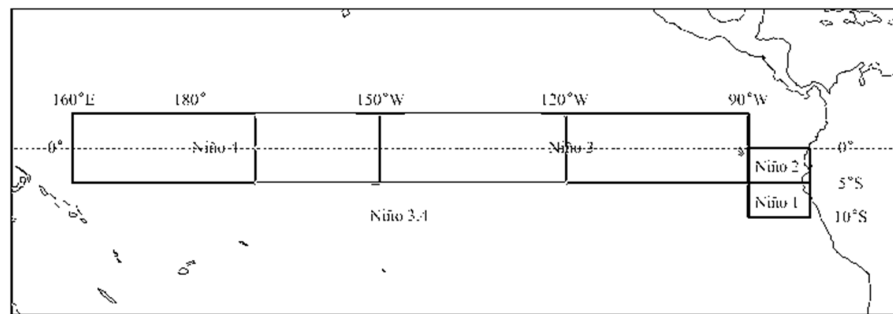
**Fig. 7** ENSO monitoring key area distribution (cited from the National Climate Center http://cmdp.ncc-cma.net/cn/index.htm).

for determining the El Niño and the La Niña events (Fig. 7, China Weather Bureau, National Climate Center). The indicators were as follows: The NINO integrated zone SSTA lasted for 6 months or more of $\geqslant 0.5$ °C (during the course of the months, there was a single month of undeclared target) as an El Niño event; An El Niño event was also defined if the district index was $\geqslant 0.5$ °C for 5 months and the sum of the indices over 5 months was $\geqslant 0.4$ °C; NINO integrated zone SSTA lasted for at least 6 months of $\leqslant -0.5$ °C (during the course of the months, there might be a single month of less than the target) as a La Niña event; if the area lasted for 5 months of $\leqslant -0.5$ °C, and the sum of the indices during 5 months of $\leqslant -0.4$ °C, it was also defined as a one-time La Niña event [24].

From the statistics, the ENSO events occurred during 1982–2014 with a total of eight El Niño events; and the El Niño years were 1982, 1983, 1986, 1987, 1991, 1992, 1994, 1997, 2002, 2006, and 2009. La Niña incidents occurred seven times; and the La Niña years were 1984, 1988, 1995-1996, 1998, 1999, 2000, 2001, 2007, 2008, 2010, 2011, and 2012. All the other years were normal years.

From 1982 to 2014, a total of 51 extreme high temperature events occurred in the Northwest Pacific, of which 13 (25.49%) occurred in El Niño years, 25 (49.02%) in La Niña years, and 13 (25.49%) in normal, non-El Niño non-La Niña, years. It could be seen that in La Niña years, extreme high temperature events were more likely to occur.

Correlation analysis was done between the number of days of extreme high temperature from 1982 to 2014 and the ENSO Index of Nino (Fig. S1). In the figure, the black bars indicated not passing 95% confidence level, and the grey bars mean passing 95% confidence level.

There were a significant negative correlation ($p = 0.0261$) between the high temperature days and Nino3 area in September, with a correlation coefficient of $R = -0.3871$, and a significant negative correlation with the Nino3.4 areas in the second half of the year (July–December) (Fig. S1 (a,b)). The Nino3 and the Nino3.4 regions located in the Central Equatorial Pacific. In another word, when the equatorial Pacific Ocean was in the cold phase of the ENSO Cycle (La Niña event), the SST would be an abnormally warm situation, and the extreme high temperatures would occur easily. In addition, this feature was also evidenced from the comparison of the extreme temperature events occurring time with the ENSO Index for each month of the Nino3.4 (Fig. S2).

From the aforementioned analyses, the extreme high temperature events are characterized by a major cycle of 3–5a, which is significantly related to the ENSO event. This may be related to the abnormality of trade winds in the ocean over the equatorial Pacific Ocean [5]. Under normal circumstances, the equatorial Pacific Ocean is prevailing in the face of the winds. With the southeastern and the northeast trade winds on each side of the equator, the equatorial Pacific surface water flows from east to west and forms surface ocean currents. This ocean current transports the warm seawater of the Pacific Ocean to the Western Pacific, causing the water level in the Western Pacific to rise and the heat to accumulate [25]. In the case that the trade wind is obviously weakened, the ocean level can be released, the surface warm water returns to the east, the sea surface in the Eastern Pacific rises, the sea surface warms up, the slope temperature layer thickens, and the El Niño phenomenon appears [26]. When the trade wind is abnormally strong, the flow of surface water from the east to the west of the equatorial Pacific will be strengthened. This will

lead to the accumulation of a larger amount of warm seawater in the Western Pacific and the occurrence of the La Niña phenomenon, which may explain the extreme high SST events during the La Niña.

In addition, large-scale air-sea interactions in the ENSO Cycle will also have important effects on SST in the Western Pacific Ocean, such as the ocean Kelvin wave and the Rossby wave. The SST in the Western Equatorial Pacific is generally high. If for some reason, the trade wind is abnormal (weakened), it can trigger an abnormal warm Kelvin wave spreading eastward. Due to the coupled air-sea interaction, this anomalous warm Kelvin wave can be strongly developed during the eastward process, eventually leading to the El Niño event. At the same time as the warm Kelvin wave, the air-sea coupling interaction will also stimulate the generation of a cold-moving Rossby wave propagating westward. On the one hand it reduces the SST of the Western Pacific, but on the other hand it reflects the cold Kelvin wave in the west bank If the trade wind is abnormal (enhanced), the cold Kelvin wave will continue to generate and transmit eastward in the Western Pacific, and it will stimulate the generation of warm Rossby waves through the coupling of sea-air interaction, similarly to the warm Kelvin wave on the eastern coast of the Equatorial Pacific. The reflected warm Rossby wave is transmitted to the Western Equatorial Pacific. On the one hand it increases the SST of the Western Equatorial Pacific, but on the other hand it reflects the warm Kelvin wave in the west bank, which prepares conditions for the next cycle [5]. This is probably related to the cycle of extreme high SST events.

**CONCLUSION**

The extreme high temperature events have monthly and interannual characteristics. Extreme high temperature events mainly concentrated during June–October, and the frequency is increasing. The number of extreme high temperature days and the duration of single extreme high temperature events were increasing gradually. The average and the maximum SST also increased. The intensity of SST in the Northwest Pacific is linearly correlated with the intensity of El Niño-Southern Oscillation. During the El Niño event, SST decreased significantly; while during the La Niña event, SST increased significantly. Hence, it could be concluded that the extreme high temperature events were more likely to occur when the Pacific equatorial cold phase (La Niña event) occurred in the ENSO Cycle. The trade winds anomaly over the Equatorial Pacific Ocean

and the massive air-sea interactions in the ENSO Cycle had an important impact on the extreme high temperature events in the Northwest Pacific.

This study mainly focused on the influence of ocean thermal factors on extreme temperature events. For future studies, it is recommended to discuss more about thermal and dynamic factors, such as low-level relative vorticity, middle tropospheric humidity, vertical wind shear, etc., and to comprehensively consider the impact of extreme temperature changes. Then, under the scenario of global warming of 1.5 °C or 2 °C, what will happen to the extreme high temperature events in the Northwest Pacific? This scientific problem is worthy of further study in the future work.

**Appendix A. Supplementary data**

Supplementary data associated with this article can be found at http://dx.doi.org/10.2306/scienceasia1513-1874.2021.051.

**REFERENCES**

1. IPCC (2011) Managing the risks of extreme events and disasters to advance climate change adaptation (SREX). Cambridge, Cambridge University, UK.
2. Thomas LF, Erich MF, Nicolas G (2018) Marine heatwaves under global warming. *Nature* **560**, 360–364.
3. Trenberth KE, Branstator GW, Karoly D, Kumar A, Lau NC, Ropelewski C (1998) Progress during toga in understanding and modeling global teleconnections associated with tropical sea surface temperatures. *J Geophys Res* **103**, 14291–14324.
4. Alexander MA, Bladé I, Newman M, Lanzante JR, Lau NC, Scott JD (2002) The atmospheric bridge: the influence of Enso teleconnections on air-sea interaction over the global oceans. *J Clim* **15**, 2205–2231.
5. Li XY, Zhai PM (2000) On indices and indicators of ENSO episodes. *Acta Meteorol Sin* **58**, 102–109.
6. Wyrtki K (1975) El Niño: the dynamic response of the equatorial Pacific ocean to atmospheric forcing. *J Phys Oceanogr* **5**, 572–584.
7. Huang RH, Zhang RH, Yan BL (2001) Dynamic effect of zonal wind abnormality on ENSO cycle in tropical West Pacific. *Sci China Ser D Earth Sci* **31**, 697–704.
8. Bejarano L, Jin FF (2006) Coexistence of equatorial coupled modes of Enso. *J Clim* **21**, 3051–3067.
9. Meng W, Wu GX (2000) Gearing between the Indo-Monsoon circulation and the Pacific-Walker circula-

tion and the ENSO part two: Numerical simulation. *Chinese J Atmos Sci* **24**, 15–25.

10. Kug JS (2006) Interactive feedback between Enso and the Indian Ocean. *J Clim* **19**, ID 6371.
11. Cravatte S, Delcroix T, Zhang D, Mcphaden M, Leloup J (2009) Observed freshening and warming of the western pacific warm pool. *Clim Dynam* **33**, 565–589.
12. Lee T, Mcphaden MJ (2010) Increasing intensity of El Niño in the central-equatorial Pacific. *Geophys Res Lett* **37**, 1–5.
13. Power S, Delage F, Chung C, Kociuba G, Keay K (2013) Robust twenty-first-century projections of El Niño and related precipitation variability. *Nature* **502**, 541–545.
14. Cai W, Borlace S, Lengaigne M, Rensch PV, Collins M, Vecchi G (2014) Increasing frequency of extreme El Nino events due to greenhouse warming. *Nat Clim Change* **4**, 111–116.
15. Reynolds RW, Smith TM, Liu C, Chelton DB, Casey KS, Schlax MG (2007) Daily high-resolution-blended analyses for sea surface temperature. *J Clim* **20**, 5473–5496.
16. Solomon S, Qin D, Manning M, Chen Z, Marquis M, Averyt KB (2007) Summary for policymakers. In: Climate change 2007: The physical science basis. Contribution of working group 1 to the fourth assessment report of the intergovernmental panel on climate change. *Comput Geom* **18**, 95–123.
17. Panmao Z, Fumin R, Qiang Z (1999) Detection of trends in China's precipitation extremes. *Acta Meteorol Sin* **57**, 208–216.
18. Jones PD, Horton EB, Folland CK, Hulme M, Parker DE, Basnett TA (1999) The use of indices to identify changes in climatic extremes. *Clim Change* **42**, 131–149.
19. Bonsal BR, Zhang X, Vincent LA, Hogg WD (2010) Characteristics of daily and extreme temperatures over Canada. *J Clim* **14**, 1959–1976.
20. Yan Z, Jones PD, Davies TD, Moberg A, Bergström H, Camuffo D (2002) Trends of extreme temperatures in Europe and china based on daily observations. *Clim Change* **53**, 355–392.
21. Qian WH, Jiao FU, Zhang WW, Xiang L (2007) Changes in mean climate and extreme climate in china during the last 40 years. *Adv Earth Sci* **22**, 673–684.
22. Ren G, Feng G (2010) Progresses in observation studies of climate extremes and changes in mainland china. *Clim Environ Res* **15**, 337–353.
23. Chen HB, Fan XH (2011) Some extreme events of weather, climate and related phenomena in 2010. *Clim Environ Res* **16**, 789–804.
24. Li XY, Zhai PM, Ren FM (2005) Redefining ENSO episodes based on changed climate references. *J Trop Meteorol* **21**, 72–78.
25. Zhai PM, Li XY, Ren FM (2003) *El Niño*, China Meteorological Press, Beijing, China.
26. Li CY (2000) *An Introduction to Climate Dynamics*, China Meteorological Press, Beijing, China.

## Appendix A. Supplementary data
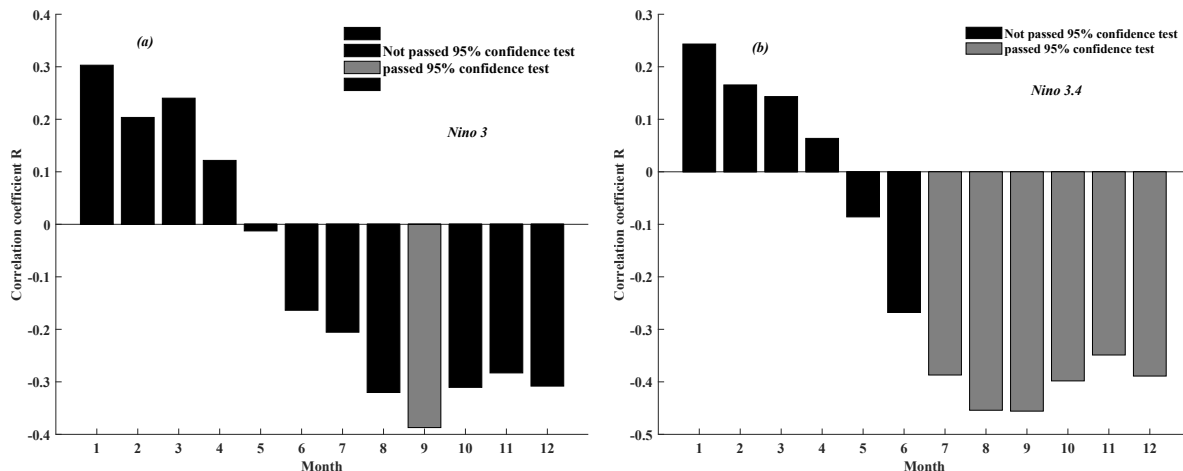


**Fig. S1** Correlation between the number of days of extreme high temperature and ENSO Index in Nino area in the Northwest Pacific during 1982–2014.
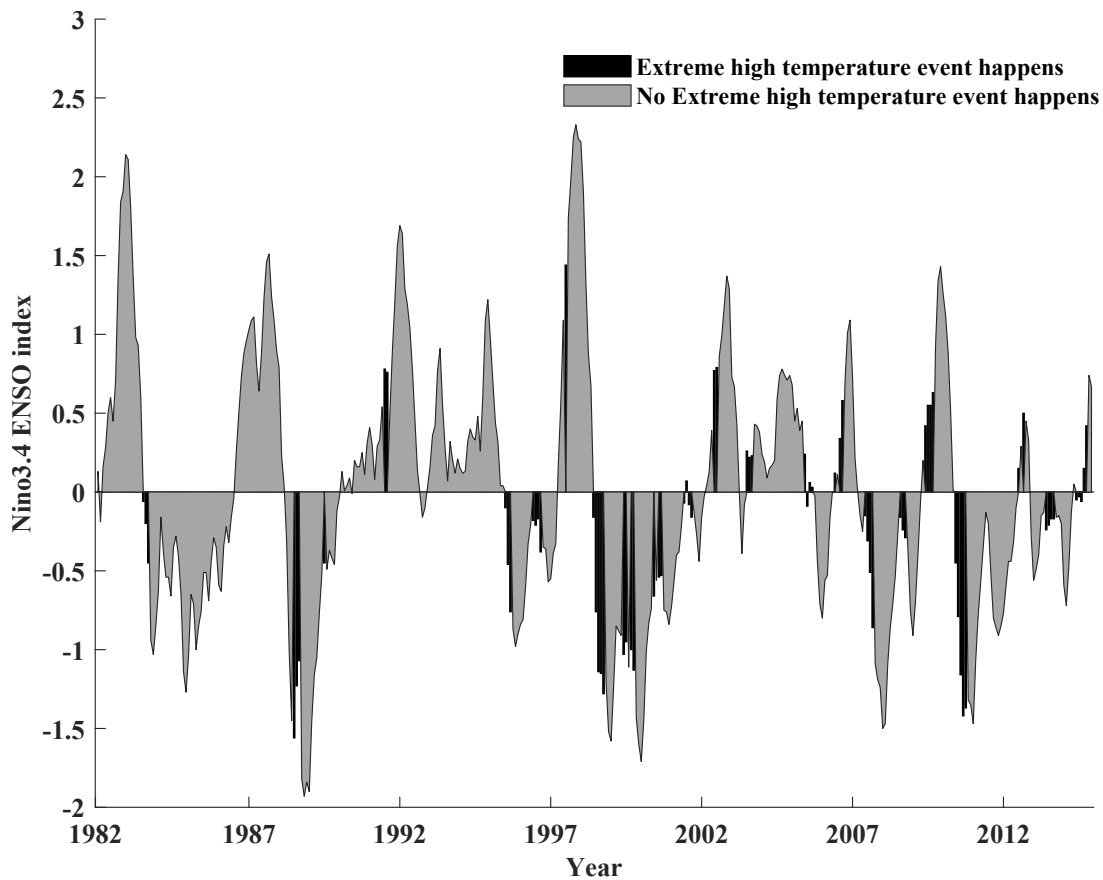


**Fig. S2** Comparison of extreme high temperature occurrence time in the Northwest Pacific and ENSO Index in Nino3.4 during 1982–2014.